Published in final edited form as:
Dev Dyn. 2009 August ; 238(8): 2095–2102. doi:10.1002/dvdy.22021.

Regional Expression of MTG Genes in the Developing Mouse Central Nervous System

Amin Alishahi, **Naoko Koyano-Nakagawa***, and **Yasushi Nakagawa***
Department of Neuroscience and Stem Cell Institute, University of Minnesota Medical School, Minneapolis, Minnesota

Abstract

Myeloid translocation gene (MTG) proteins are transcriptional repressors that are highly conserved across species. We studied the expression of three members of this gene family, *MTGR1*, *MTG8*, and *MTG16* in developing mouse central nervous system by in situ hybridization. All of these genes are detected as early as embryonic day 11.5. Because these genes are known to be induced by proneural genes during neurogenesis, we analyzed the expression of *MTG* genes in relation to two proneural genes, *Neurog2* (also known as *Ngn2* or *Neurogenin 2*) and *Ascl1* (also known as *Mash1*). While *MTGR1* are generally expressed in regions that also express *Neurog2*, *MTG8* and *MTG16* expression is associated more tightly with that of *Ascl1*-expressing neural progenitor cells. These results suggest the possibility that expression of *MTG* genes is differentially controlled by specific proneural genes during neurogenesis.

Keywords

MTG8; MTG16; MTGR1; CBFA2T1; CBFA2T2; CBFA2T3; ETO; ETO-2; ETO-R; EHT; Neurog2; Ngn2; Neurogenin; Ascl1; Mash1; achaete-scute homolog; neurogenesis; differentiation; neuronal progenitor; spinal cord; telencephalon; diencephalon; thalamus; retina; central nervous system; CNS; lineage tracing; basic helix-loop-helix; bHLH; transcription factor; transcriptional repressor; histone deacetylase; HDAC; N-CoR; Sin3A; AML; acute myeloid leukemia; Nvy; nervy

INTRODUCTION

MTGR1 (also known as ETOR/Cbfa2t2/EHT), MTG8 (also ETO/Cbfa2t1), and MTG16 (also ETO-2/Cbfa2t3/MTGR2) are members of the MTG (myeloid translocation gene) protein family. These proteins are transcriptional repressors that are highly conserved across species. A large body of research on the function of MTG proteins has been done focusing on oncogenesis, in which chromosomal translocation of *MTG* genes was associated with acute myeloid leukemia and breast cancer (for reviews, see Davis et al., 2003; Hug and Lazar, 2004; Rossetti et al., 2004). It was believed that MTG proteins are expressed rather ubiquitously, because Northern blot analysis showed that a large number of organs express *MTG* transcripts (Miyoshi et al., 1993; Wolford and Prochazka, 1998; Morohoshi et al., 2000; Calabi et al., 2001). However, each transcript seems to be expressed in specific cell types. For example, *MTG8* mutant mice showed impaired midgut development, whereas *MTGR* mutant mice failed to maintain secretory cell lineage in the small intestine (Calabi et al., 2001, Amann et al., 2005). Specific interactions of MTG proteins with Delta/Notch signaling

*Correspondence to: Yasushi Nakagawa or Naoko Koyano-Nakagawa, Department of Neuroscience and Stem Cell Institute, University of Minnesota Medical School, Minneapolis, MN 55455. umn.edu or koyano@umn.edu.

and Wnt signaling pathways have also been suggested (Cao et al., 2002; Wildonger and Mann, 2005; Moore et al., 2008).

During early stages of neurogenesis, *MTG* genes are strongly induced by a number of proneural basic helix-loop-helix (bHLH) proteins including XNGNR-1, Xath3, Xath5, and XNeuroD, suggesting their role as a widely employed regulator of neuronal differentiation (Cao et al., 2002; Koyano-Nakagawa and Kintner, 2005; Logan et al., 2005; Seo et al., 2007). In the mouse telencephalon, *MTG8* was identified as a potential target of Neurog2 (also known as Ngn2 or Neurogenin 2; Gohlke et al., 2008). In addition, a later role of MTGR1 as a repressor of β1 integrin-dependent neurite outgrowth via regulation of EGF and FGF expression was recently reported (Ossovskaya et al., 2009). In this report, we performed a detailed analysis of expression for each of the three members of the *MTG* family during neurogenesis in mice. Interestingly, we noticed that the domains of *MTGR1* expression generally coincided with that of *Neurog2*, whereas expression of *MTG8* and *MTG16* was largely confined to the lineage of progenitor cells expressing *Ascl1* (also known as *Mash1*). This correlation was further confirmed by analyzing gene expression in transgenic mice that express EGFP under the control of *Ascl1* gene. These findings suggest that during neural development, each of the *MTG* genes may play specific roles in modulating the activity of bHLH transcription factors.

RESULTS AND DISCUSSION

Expression in the Telencephalon

MTGR1—*MTGR1* started to be clearly detectable in the dorsal telencephalon at embryonic day 10.5 (E10.5). Expression was highly enriched in the preplate (PP, Fig. 1A), where newly formed neurons reside. At this stage, *Neurog2* was expressed in the ventricular zone (VZ) in a salt-and-pepper pattern (Fig. 1B; Gradwohl et al., 1996). *MTGR1* and *Neurog2* appeared to share the same ventral border (Fig. 1A,B, arrow), and were not detected in the ventral telencephalon. At E11.5, both *MTGR1* and *Neurog2* continued to be expressed in the dorsal telencephalon. *MTGR1* was now more broadly expressed across the cortical wall (Fig. 2A–C, Cx), similar to *Neurog2* (Fig. 2E–G, Cx). In addition, very weak *MTGR1* expression was detected in the ventral telencephalon, including the lateral (LGE) and caudal (CGE) ganglionic eminences (Fig. 2A,B). At E13.5, *MTGR1* was expressed in the dorsal telencephalon with a clear laminar preference (Fig. 3A–D). A high expression was found in the PP (Fig. 3A–D) and the subventricular zone (SVZ, Fig. 3A–D). Scattered cells in the VZ also expressed *MTGR1* (Fig. 3A–D). At this stage, *Neurog2* was most densely expressed in the VZ (Fig. 3E–H), with less dense expression in the SVZ (Fig. 3E–H;Gradwohl et al., 1996). High-magnification images on adjacent sections show that there is some overlap of expression between *MTGR1* and *Neurog2* in the SVZ (Fig. 3D,H). At E15.5, *MTGR1* was down-regulated in the neocortex; only the medial (Fig. 4B, mCx) and lateral (Fig. 4A,B, lCx) parts of the dorsal telencephalon continued to express *MTGR1*. The same pattern of expression continued to postnatal day 0 (P0, not shown).

MTG8—*MTG8* started to be expressed at E10.5 in the mantle zone of the ventral telencephalon (Fig. 1C, LGE and medial ganglionic eminence, MGE), while it was not detected in the cortex. At E11.5, *MTG8* was strongly expressed in the mantle zone of MGE, LGE, and CGE (Fig. 2I,J), but it was undetectable in the dorsal telencephalon (Fig. 2I–K, Cx). This ventral-specific expression was similar to that of *Ascl1*, although *Ascl1* was only detected in the VZ, and not in the mantle zone (Fig. 2Q,R). At E13.5, *MTG8* was still expressed in the ventral telencephalic mantle zone, which is derived from the MGE and LGE (Fig. 3I,J, double arrows). In addition, starting at this stage, *MTG8* was also clearly detected in the cortical PP (Fig. 3I,J). These cells are either derived from the dorsal telencephalon or have migrated from the MGE and CGE (Metin et al., 2006;Butt et al., 2005). At E15.5, *MTG8* expression in the cortex was decreased

in general, with the exception of the medial (Fig. 4C,D, mCx) and lateral (Fig. 4C, lCx) parts, similar to *MTGR1*. The same pattern was found at P0 (not shown).

MTG16—Similar to *MTG8, MTG16* was also expressed in the mantle zone of the ganglionic eminences starting at E10.5 (Fig. 1D). Unlike *MTG8*, the level of expression was much higher in the MGE than in the LGE or CGE. The pattern at E11.5 was essentially the same as E10.5 (Fig. 2M,N). Similar to *MTG8, MTG16* was detected in the cortical PP at E13.5 (Fig. 3K). At E14.5, after the splitting of the PP by the cortical plate, we saw both the marginal zone (Fig. 4I) and presumptive subplate (Fig. 4I, arrowheads) with significant levels of *MTG16* expression. At E15.5, *MTG16* was still expressed in the marginal zone (Fig. 4J) and the subplate (Fig. 4J, arrowheads), but expression was higher in the lateral part of the telencephalon (Fig. 4E,F, lCx). At P0, *MTG16* was largely down-regulated in the cortex (data not shown). In contrast, at E15.5, *Neurog2* expression was largely restricted to the VZ (Fig. 4H,K) and SVZ (Fig. 4H,K), while the cortical plate had much lower expression (Fig. 4H).

Expression in the Diencephalon

MTGR1—Strong expression of *MTGR1* in the caudal diencephalon, including the thalamus (Fig. 2B,C, Th) and the rostral pretectum (Fig. 2D, rPT), started at E11.5. Weak expression continued rostrally into the prethalamus (Fig. 2C, PTh). At E13.5, when a prominent mantle zone was formed in the entire diencephalon, *MTGR1* was detected along the outer edge of the VZ in the pretectum (not shown), the thalamus (Fig. 3C, Th, shown by arrowheads), and the prethalamus (Fig. 3C, PTh). By E15.5, *MTGR1* expression was down-regulated in these regions (Fig. 4B). In addition to the above regions, at both E11.5 and E13.5, *MTGR1* was expressed in the eminentia thalami, which is located dorsal to the prethalamus (Figs. 2B and 3C, EMT) (Puelles and Rubenstein, 2003), as well as in the VZ, which is close to the future dorsomedial nucleus of the hypothalamus (Figs. 2B and 3C, HT). Within most of the *MTGR1*-expressing regions in the diencephalon, *Neurog2* was expressed in the VZ (thalamus, Figs. 2F,G and 3G, Th; eminentia thalami, Figs. 2F and 3G, EMT; rostral pretectum, Fig. 2H, rPT), except in the prethalamus (Fig. 2G, PTh). In addition to the VZ, the mantle zone of the thalamus (Figs. 2F, 3G, double arrows) and a part of the hypothalamus (Figs. 2F, 3G, triple arrows) also showed *Neurog2* expression at E11.5 and E13.5 (Gradwohl et al., 1996; Nakagawa and O'Leary, 2001). Thus, within the diencephalon, *MTGR1* and *Neurog2* showed a significant overlap in expression areas. In addition, where these two genes overlap, *Neurog2* expression always preceded the induction of *MTGR1*.

MTG8—*MTG8* expression in the mantle zone of the thalamus was first detected at E11.5 (Fig. 2K,L, Th). At this stage, *MTG8* was also expressed in the dorso-caudal part of the hypothalamus (paraventricular region; Fig. 2K, HT) where *Ascl1* expression was strong and *Neurog2* was absent (Fig. 2G,K,S). Unlike *MTGR1* and *MTG16*, expression of *MTG8* in the pretectum was not clearly detected (Fig. 2L, rPT). At E13.5, there was a gradient of *MTG8* expression in the thalamic mantle zone, which was higher in the caudo-dorsal region (Fig. 3J, double arrowheads) than in the rostro-ventral region (Fig. 3J, single arrowhead) (see Vue et al., 2007, for axial nomenclature of the thalamus). This graded pattern of *MTG8* expression in the thalamic mantle zone was already observed at E12.5 on sagittal sections (see Fig. 7F, Th), and continued to E15.5 (Fig. 4D, caudo-dorsal part is shown by double arrowheads, whereas rostro-ventral part is indicated by a single arrowhead). In addition to the thalamus and paraventricular hypothalamus, *MTG8* was also expressed in the reticular nucleus of the prethalamus (Fig. 4C, RT) and subthalamic nucleus of the hypothalamus (Fig. 4D, STh). At P0, this region-specific expression pattern of *MTG8* was still largely preserved (not shown).

MTG16—At E11.5, *MTG16* was expressed weakly and broadly in the thalamic mantle zone. However, in the most rostro-ventral part of the thalamus, *MTG16* was detected in a narrow

band (Fig. 2O), which is immediately lateral to the band of *Ascl1*-expressing domain in the thalamus (Fig. 2S, pTH-R). We previously showed that this *Ascl1*-expressing progenitor domain, termed pTH-R, gives rise to thalamic nuclei such as intergeniculate leaflet and the ventral lateral geniculate nucleus (Vue et al., 2007). In addition to the thalamus, *MTG16* was strongly expressed in the caudal pretectum (Fig. 2P, cPT), which also expressed *Ascl1* (Fig. 2T). At E15.5 and later, *MTG16* was expressed in the ventral lateral geniculate nucleus and intergeniculate leaflet (Fig. 4G, IGL/vLG), which are derived from the Ascl1-expressing progenitor domain, pTH-R (Vue et al., 2007). We also found that *MTG16* was expressed in the paraventricular nucleus of the thalamus (Fig. 4G, PV).

Expression in the Retina

MTGR1—In the retina, *Neurog2* started to show a distinctive salt-and-pepper expression pattern in progenitor cells at E11.5 (Fig. 5A). Coinciding with this expression, *MTGR1* started to be detectable also at E11.5 (Fig. 5C). Both genes are expressed highly in the central part of the retina (shown by arrows). At E13.5, we detected robust expression of *MTGR1* as well as *Neurog2* in the VZ (Fig. 6A,C). In addition, *MTGR1* was expressed in the ganglion cell layer as well (Fig. 6A, GCL). At E15.5, *MTGR1* was still expressed in the retina, but was further enriched in the ganglion cell layer (Fig. 6B, GCL), where *Neurog2* was not detected (Fig. 6D, Gradwohl et al., 1996). The expression level appeared to be decreased at P0 (not shown). Thus, the temporal and spatial expression patterns of *MTGR1* and *Neurog2* in the retina are consistent with the possibility that Neurog2 regulates the expression of *MTGR1*.

MTG8 and MTG16—*MTG8* expression was first detected in the ganglion cell layer at E13.5 (Fig. 6E, GCL), but not in the VZ. This pattern continued at E15.5 (Fig. 6F). *MTG16* expression in the retina was first detected at E13.5 (Fig. 6G). The level of expression appeared to be higher in the ganglion cell layer than in the VZ, but the difference was not as clear as it was for *MTG8* expression. At E15.5, *MTG16* expression was clearly enriched in the ganglion cell layer (Fig. 6H, GCL). Both *MTG8* and *MTG16* continued to be expressed in the ganglion cell layer at P0 (data not shown). Scattered expression of *Ascl1* was first detected at E11.5 by immunohistochemistry (Fig. 5D) and in situ hybridization (Fig. 5B). With double labeling, it was found that Ascl1 was expressed in a largely non-overlapping population with Neurog2 (Fig. 5D), which was consistent with a previous report (Marquardt et al., 2001). *Ascl1* expression was maintained at E13.5 and E15.5, but was more highly expressed in the VZ than in the ganglion cell layer (Fig. 6I,J). At P0, *Ascl1* was still expressed in a pattern similar to E15.5 (not shown).

Expression in the Midbrain and Hindbrain

On sagittal sections at E12.5, *MTGR1* was expressed broadly in the middle layer of the midbrain (Fig. 7A,B, arrowhead) and the dorsal hindbrain near the 4th ventricle (Fig. 7A,B, double arrows). *Neurog2* was also expressed in the VZ of similar regions (Fig. 7C,D, arrowhead and double arrows). *MTG8* and *MTG16* were both expressed broadly in the midbrain and hindbrain, including much of the ventral midbrain (Fig. 7E–H, double arrows) as well as part of the hindbrain (Fig. 7E–H, HB). *MTGR1*, *MTG8*, and *MTG16* were also strongly expressed in the cerebellar primordium, outside the VZ (Fig. 7B,E–H, Cb), whereas *Ascl1* and *Neurog2* were both expressed within the VZ. In summary, in the midbrain and hindbrain including the cerebellum, *MTG* genes were broadly expressed with significant overlaps. Similarly, *Ascl1* and *Neurog2* were expressed in the VZ with overlapping patterns (Fig. 7C,D,I,J).

Expression in the Spinal Cord

MTGR1—At E10.5, we detected *MTGR1* in the most dorsal progenitor population, presumably the dp1 domain (Fig. 8A, arrowhead; Helms and Johnson, 2003;Zhuang and

Sockanathan, 2006). *Neurog2*, which is known to be expressed in the dp2 domain, was detected immediately ventral to the *MTGR1*-expressing domain on adjacent sections (Fig. 8C, arrow and arrowhead). *MTGR1* was also expressed more ventrally; the dorso-ventral level of this expression domain coincided with that of *Neurog2* (Fig. 8A,C, double arrows). In this ventral domain, *Neurog2* expression extended more medially than *MTGR1*. At E12.5, *MTGR1* expression became broader, covering most of the dorso-ventral extent, but with weaker expression ventrally. This dorso-ventral distribution of *MTGR1*-positive cells was very similar to that of *Neurog2* (Figs. 8B,D, 9A,B, arrowheads).

MTG8 and MTG16—*MTG8* expression was found broadly in the mantle zone of the dorsal spinal cord already at E10.5 (Fig. 8E, arrowhead). Motor neurons also had strong expression (Fig. 8E, arrow). At E12.5, expression became more diffuse and occupied most of the dorsal horn of the spinal cord (Fig. 8F, arrow). Expression in motor neurons became weaker at this stage. *MTG16* was expressed in a pattern similar to *MTG8* in the spinal cord both at E10.5 and E12.5 (Fig. 8G,H, arrow and arrowhead). At E10.5, *Ascl1* was expressed in a broad dorsal domain that encompasses dp3 to dp5 (Fig. 8I, arrowhead) (Helms and Johnson, 2003;Zhuang and Sockanathan, 2006). At E12.5, expression became weak. In order to further evaluate the possible correlation of the expression of *MTG* genes and proneural genes, we did in situ hybridization and immunohistochemistry on *Ascl1-BAC-EGFP* mice at E11.5. We find that in the ventral spinal cord, *MTG8* expression correlated well with the *Ascl1* lineage in the V2 interneuron domain (Fig. 9D,F, arrow). In the ventral spinal cord, the expression of Neurog2 and Ascl1 was mutually exclusive at E11.5 (Fig. 9C, arrow and double arrows). In the dorsal spinal cord, the expression and lineage of Neurog2 and Ascl1 overlapped more extensively than in the ventral cord (Fig. 9B,C, arrowhead). However, the broad expression pattern and medio-lateral boundary of *MTGR1* expression correlated better with that of Neurog2 than with Ascl1 (compare Fig. 9A,B,F).

Summary of MTG Gene Expression

Our analysis of the expression of the *MTG* genes in the developing mouse CNS reveals that the three members of the *MTG* gene family are expressed in overlapping but distinctive populations of cells. Interestingly, *MTG* genes can be induced by over-expression of proneural bHLH genes in the neural tube (Cao et al., 2002; Koyano-Nakagawa and Kintner, 2005; Logan et al., 2005; Seo et al., 2007; Gohlke et al., 2008), and bHLH genes such as *Neurog2* and *Ascl1* show limited overlap in expression within the developing central nervous system (Gradwohl et al., 1996). Thus, it is possible that each bHLH proneural gene preferentially activates the expression of the three *MTG* genes. We compared the expression of *MTG* genes with that of *Neurog2* and *Ascl1*, and found that the spatial and temporal expression patterns of all three members of the *MTG* gene family were compatible with their status as downstream targets of *Neurog2* and/or *Ascl1*. *MTGR1* expression was generally associated with that of *Neurog2* in the dorsal telencephalon as well as in the thalamus and rostral pretectum. The retina and ventral spinal cord also showed some overlap. In each of these shared expression domains, *MTGR1* expression appeared to immediately follow the onset of *Neurog2*, but was generally expressed only transiently. Few domains in the mantle zone continued to express *MTGR1* beyond late embryonic stages. In contrast, *MTG8* and *MTG16* generally overlapped heavily with *Ascl1* expression domains. *MTG16* was particularly tightly linked to *Ascl1* expression in the ventral telencephalon and diencephalon. *MTG16* expression was still detectable at E15.5 and P0 in many regions (e.g., telencephalon, retina, ventral lateral geniculate nucleus). *MTG8* was continuously expressed in most of the postmitotic cell populations that express it. These results suggest that *Neurog2* and *Ascl1* may indeed have preferential regulation on different *MTG* genes. Further investigations are needed to reveal the significance of this specificity. We recently observed that all members of the MTG protein family inhibit transcriptional activity of proneural bHLH proteins (Aaker et al., unpublished observation).

Temporal and spatial specificity of *MTG* expression found in chick and *Xenopus* (Koyano-Nakagawa and Kintner, 2005) and in mice (this study) suggests that each MTG protein might have specific bHLH targets to inhibit.

EXPERIMENTAL PROCEDURES

Animals

Care and experimentation on mice were done in accordance with the Institutional Animal Care and Use Committee of the University of Minnesota. Noon of the day on which the vaginal plug was found was counted as embryonic day 0.5 (E0.5). Stages of early embryos were confirmed by morphology (Kaufman, 1992). CD1/ICR mice (Charles River) and *Ascl1-BAC-EGFP mice* (MMRRC stock number 000295-UNC, Gong et al., 2003) were used.

In Situ Hybridization and Immunohistochemistry

In situ hybridization and immunohistochemistry were performed as described (Vue et al., 2007). Antibodies used are: rabbit anti-GFP (Molecular Probes), goat anti-Neurog2 (Santa Cruz Biotechnology, sc-19233), and mouse anti-Ascl1 (BD Pharmingen, 556604). For each embryonic stage, different layers of the cortex were assessed by (1) DAPI staining; VZ, SVZ, and CP have high cell density compared with SP (subplate)/IZ (intermediate zone) and MZ/PP, and (2) immunostaining of βIII-tubulin, calretinin, and phospho-histone H3 (PH3); βIII-tubulin is in high density in CP, calretinin is strongly expressed in MZ/PP, and PH3 is expressed at the ventricular surface as well as in the SVZ (data not shown).

Probes

A template for MTG8 probe was obtained by PCR-amplifying the 3′UTR based on published sequence (bases 1,318 –2,363 of NCBI D32007) from E12.5 mouse spinal cord cDNA. The fragment was subcloned into pBSII and confirmed by sequencing. Clones of mMTG16b/CBFA2T3 (CA749581) and mMTGR1/CBFA2T2h (6405896) were purchased from the I.M.A.G.E. Consortium.

Acknowledgments

This work was funded in part by the National Institute of Health (MH078998 to N.K-N and NS049357 to Y.N.). DNA sequence analyses were done using resources of the Supercomputing Institute at the University of Minnesota. We thank members of the Nakagawa and Koyano Labs for discussion and help.

Grant sponsor: National Institute of Health; Grant numbers: MH078998 and NS049357.

References

Amann JM, Chyla BJI, Ellis TC, Martinez A, Moore AC, Franklin JL, McGhee L, Meyers S, Ohm JE, Luce KS, Ouelette AJ, Washington MK, Thompson MA, King D, Gautam S, Coffey RJ, White-head RH, Hiebert SW. Mtgr1 is a transcriptional corepressor that is required for maintenance of the secretory cell lineage in the small intestine. Mol Cell Biol 2005;25:9576 –9585. [PubMed: 16227606]

Butt SJ, Fuccillo M, Nery S, Noctor S, Kriegstein A, Corbin JG, Fishell G. The temporal and spatial origins of cortical interneurons predict their physiological subtype. Neuron 2005;48:591– 604. [PubMed: 16301176]

Calabi F, Pannell R, Pavloska G. Gene targeting reveals a crucial role for MTG8 in the gut. Mol Cell Bio 2001;21:5658 –5666. [PubMed: 11463846]

Cao Y, Zhao H, Grunz H. XETOR regulates the size of the proneural domain during primary neurogenesis in Xenopus laevis. Mech Dev 2002;119:35– 44. [PubMed: 12385752]

Davis JN, McGhee L, Meyers S. The ETO (MTG8) gene family. Gene 2003;303:1–10. [PubMed: 12559562]

Gohlke JM, Armant O, Parham FM, Smith MV, Zimmer C, Castro DS, Nguyen L, Parker JS, Gradwohl G, Portier CJ, Guillemot F. Characterization of the proneural gene regulatory network during mouse telencephalon development. BMC Biol 2008;6:15. [PubMed: 18377642]

Gong S, Zheng C, Doughty ML, Losos K, Didkovsky N, Schambra UB, Nowak NJ, Joyner A, Leblanc G, Hatten ME, Heintz N. A gene expression atlas of the central nervous system based on bacterial artificial chromosomes. Nature 2003;425:917–925. [PubMed: 14586460]

Gradwohl G, Fode C, Guillemot F. Restricted expression of a novel murine atonal-related bHLH protein in undifferentiated neural precursors. Dev Biol 1996;180:227–241. [PubMed: 8948587]

Helms AW, Johnson JE. Specification of dorsal spinal cord interneurons. Curr Opin Neurobiol 2003;13:42– 49. [PubMed: 12593981]

Hug BA, Lazar MA. ETO interacting proteins. Oncogene 2004;23:4270 – 4274. [PubMed: 15156183]

Kaufman, MH. Atlas of Mouse Development. Academic Press; 1992. p. 512

Koyano-Nakagawa N, Kintner C. The expression and function of MTG/ETO family proteins during neurogenesis. Dev Biol 2005;278:22–34. [PubMed: 15649458]

Logan MA, Steele MR, Van Raay TJ, Vetter ML. Identification of shared transcriptional targets for the proneural bHLH factors Xath5 and XNeuroD. Dev Biol 2005;285:570 –583. [PubMed: 16112102]

Marquardt T, Ashery-Padan R, Andrejewski N, Scardigli R, Guillemot F, Gruss P. Pax6 is required for the multipotent state of retinal progenitor cells. Cell 2001;105:43–55. [PubMed: 11301001]

Metin C, Baudoin JP, Rakic S, Parnavelas JG. Cell and molecular mechanisms involved in the migration of cortical inter-neurons. Eur J Neurosci 2006;23:894–900. [PubMed: 16519654]

Miyoshi H, Kozu T, Shimizu K, Enomoto K, Maseki N, Kaneko Y, Kamada N, Ohki M. The t(8;21) translocation in acute myeloid leukemia results in production of an AML1-MTG8 fusion transcript. Embo J 1993;12:2715–2721. [PubMed: 8334990]

Moore AC, Amann JM, Williams CS, Tahinci E, Farmer TE, Martinez JA, Yang GY, Luce KS, Lee E, Hiebert SW. Myeloid translocation gene family members associate with T-cell factors (TCFs) and influence TCF-dependent transcription. Mol Cell Biol 2008;28:977–987. [PubMed: 18039847]

Morohoshi F, Mitani S, Mitsuhashi N, Kitabayashi I, Takahashi E, Suzuki M, Munakata N, Ohki M. Structure and expression pattern of a human MTG8/ETO family gene, MTGR1. Gene 2000;241:287–295. [PubMed: 10675041]

Nakagawa Y, O'Leary DD. Combinatorial expression patterns of LIM-home-odomain and other regulatory genes parcellate developing thalamus. J Neurosci 2001;21:2711–2725. [PubMed: 11306624]

Ossovskaya VS, Dolganov G, Basbaum AI. Loss of function genetic screens reveal MTGR1 as an intracellular repressor of beta1 integrin-dependent neurite outgrowth. J Neurosci Methods 2009;177:322–333. [PubMed: 19026687]

Puelles L, Rubenstein JL. Forebrain gene expression domains and the evolving prosomeric model. Trends Neurosci 2003;26:469 – 476. [PubMed: 12948657]

Rossetti S, Hoogeveen AT, Sacchi N. The MTG proteins: chromatin repression players with a passion for networking. Genomics 2004;84:1–9. [PubMed: 15203199]

Seo S, Lim JW, Yellajoshyula D, Chang LW, Kroll KL. Neurogenin and NeuroD direct transcriptional targets and their regulatory enhancers. EMBO J 2007;26:5093–5108. [PubMed: 18007592]

Vue TY, Aaker J, Taniguchi A, Kazemzadeh C, Skidmore JM, Martin DM, Martin JF, Treier M, Nakagawa Y. Characterization of progenitor domains in the developing mouse thalamus. J Comp Neurol 2007;505:73–91. [PubMed: 17729296]

Wildonger J, Mann RS. Evidence that nervy, the Drosophila homolog of ETO/MTG8 promotes mechanosensory organ development by enhancing Notch signaling. Dev Biol 2005;286:507–520. [PubMed: 16168983]

Wolford JK, Prochazka M. Structure and expression of the human MTG8/ETO gene. Gene 1998;212:103–109. [PubMed: 9661669]

Zhuang B, Sockanathan S. Dorsal-ventral patterning: a view from the top. Curr Opin Neurobiol 2006;16:20 –24. [PubMed: 16337785]

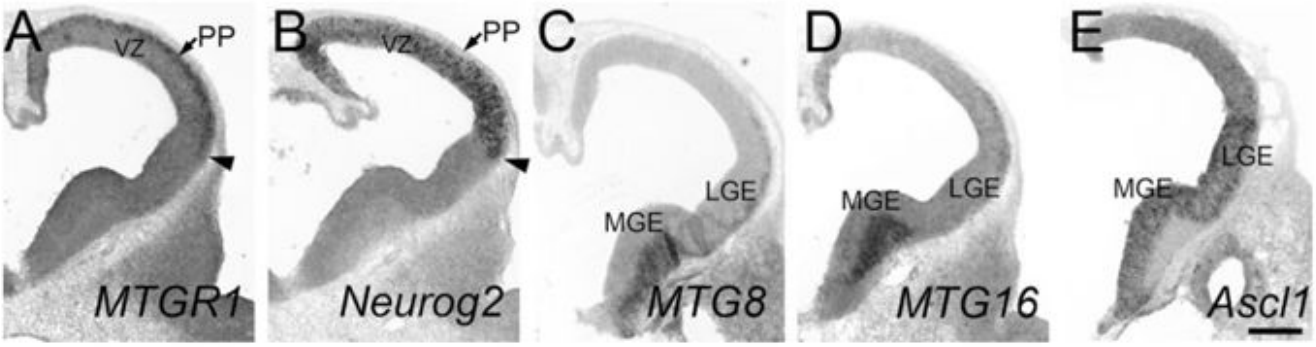

Fig. 1.

Telencephalon at E10.5. Adjacent frontal sections are shown. Midline is to the left. In situ hybridization for *MTGR1* (**A**), *Neurog2* (**B**), *MTG8* (**C**), *MTG16* (**D**), and *Ascl1* (**E**) is shown. PP, preplate; VZ, ventricular zone. Scale bar = 200 μm.

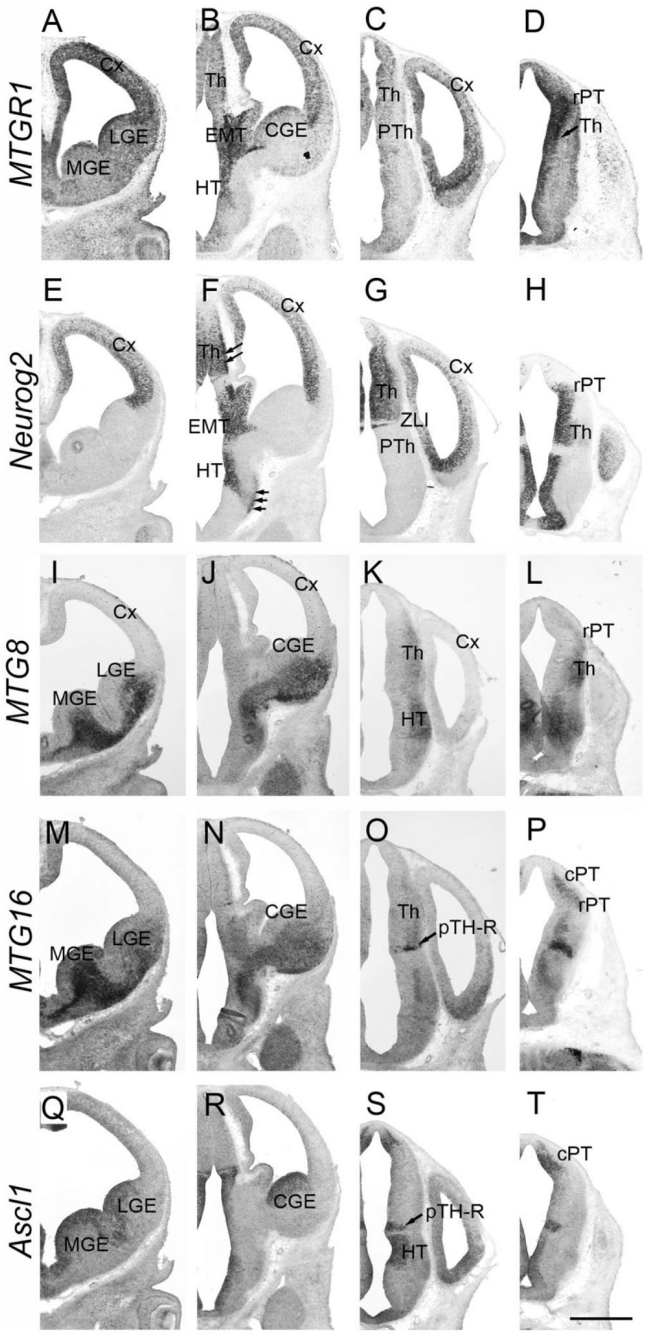

Fig. 2.

Forebrain at E11.5. Frontal sections are shown. Sections in the same column are adjacent to each other. Left columns are more frontal than right columns. Midline is to the left. In situ hybridization for *MTGR1* (**A–D**), *Neurog2* (**E–H**), *MTG8* (**I–L**), *MTG16* (**M–P**), and *Ascl1* (**Q–T**) is shown. Cx, cortex; MGE, medial ganglionic eminence; LGE, lateral ganglionic eminence; CGE, caudal ganglionic eminence; EMT, eminentia thalami; HT, hypothalamus; rPT, rostral pretectum; cPT, caudal pretectum; Th, thalamus; pTH-R, rostral thalamic progenitor domain; ZLI, zona limitans intrathalamica. Scale bar = 500 μm.

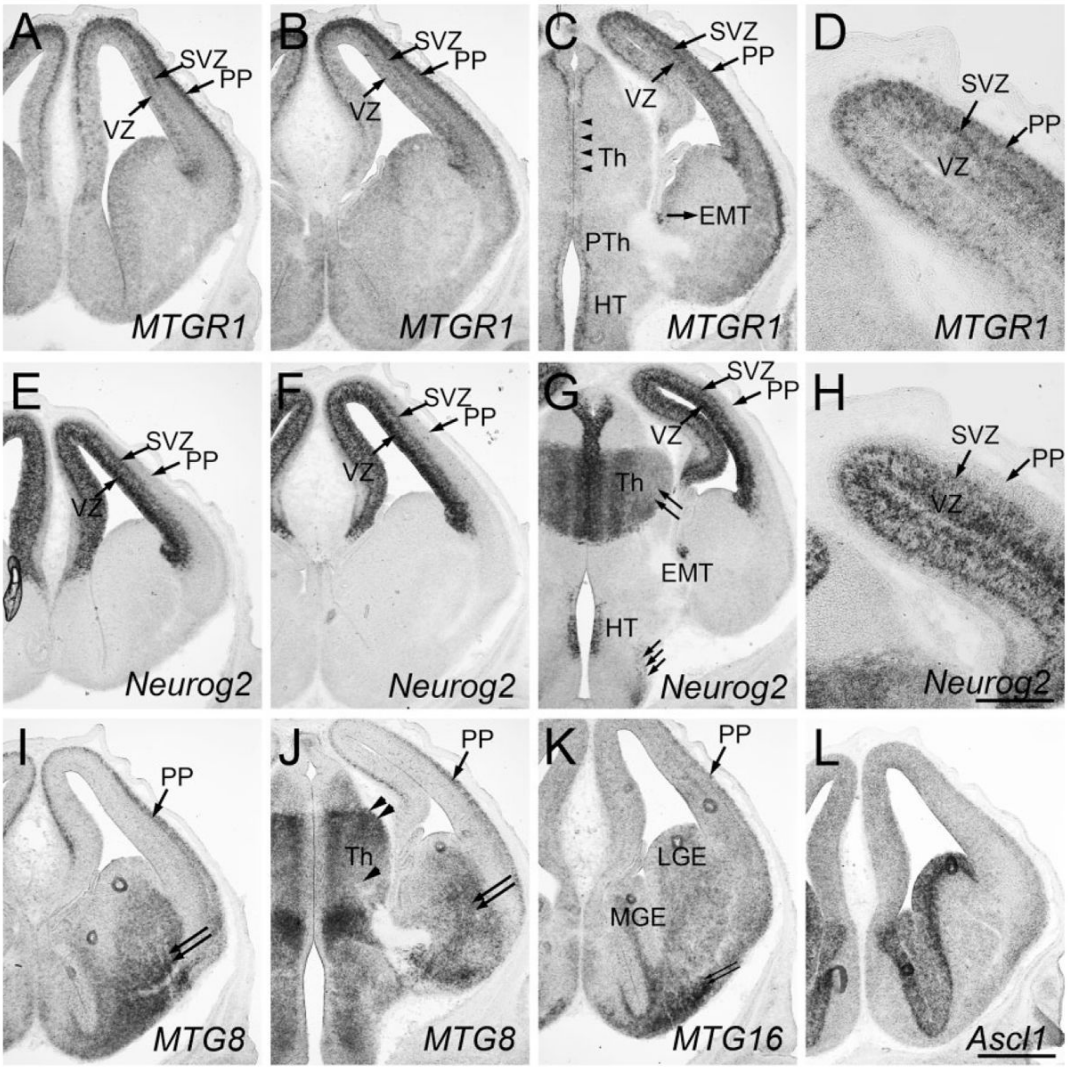

Fig. 3.

Forebrain at E13.5. Frontal sections are shown. A and E, B and F, C and G are adjacent sections. D and H are high-magnification views of C and G, respectively. Midline is to the left. In situ hybridization for *MTGR1* (**A–D**), *Neurog2* (**E–H**), *MTG8* (**I,J**), *MTG16* (**K**), and *Ascl1* (**L**) is shown. PP, preplate; SVZ, subventricular zone; VZ, ventricular zone; MGE, medial ganglionic eminence; LGE, lateral ganglionic eminence; Th, thalamus; EMT, eminentia thalami; HT, hypothalamus. Scale bar = 200 μm for D,H and 500 μm for other panels.

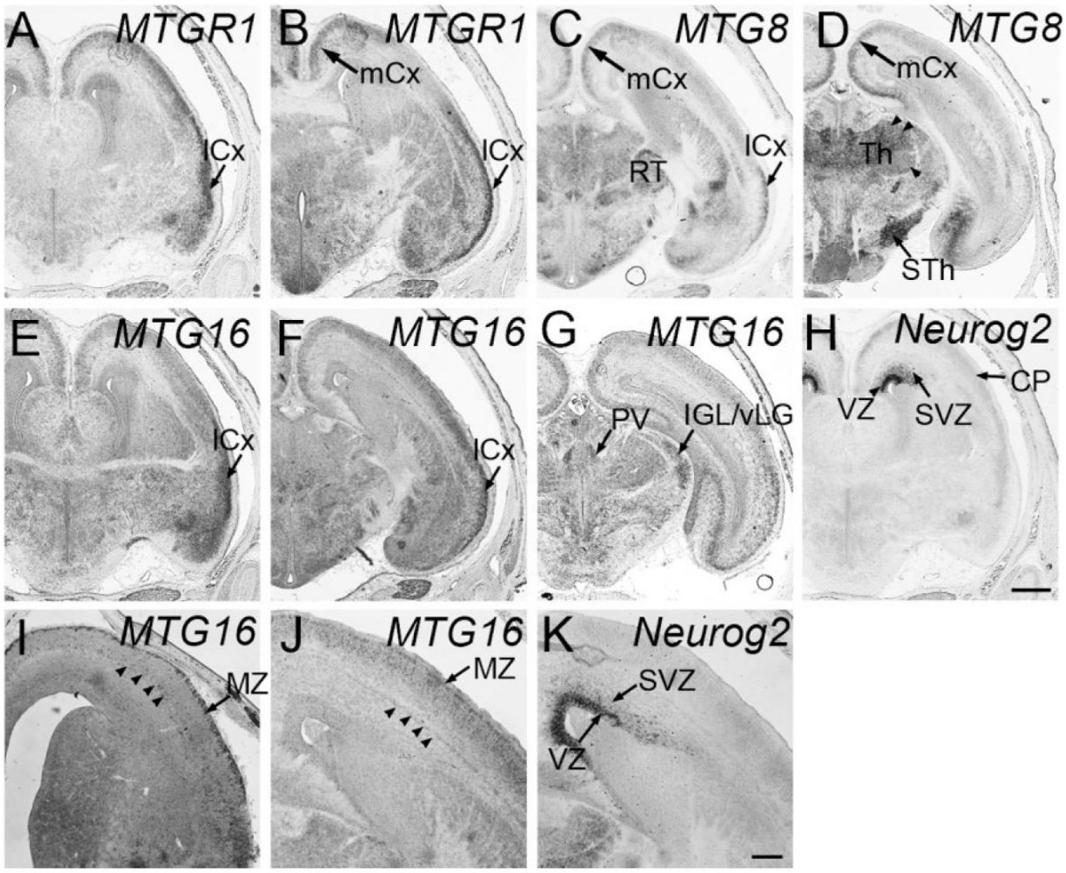

Fig. 4.

Forebrain at E14.5 and E15.5. Frontal sections are shown. A–H, J,K are from E15.5, and I is from an E14.5 embryo. Midline is to the left. In situ hybridization for *MTGR1* (**A,B**), *MTG8* (**C,D**), *MTG16* (**E–G, I,J**), *Neurog2* (**H,K**). lCx, lateral cortex; mCx, medial cortex; RT, reticular nucleus; Th, thalamus; STh, subthalamic nucleus; PV, paraventricular nucleus of the thalamus; IGL/vLG, inter-geniculate leaflet/ventral lateral geniculate nucleus; VZ, ventricular zone; SVZ, subventricular zone. Scale bar = 500 μm for A–H, 200 μm for I–K.

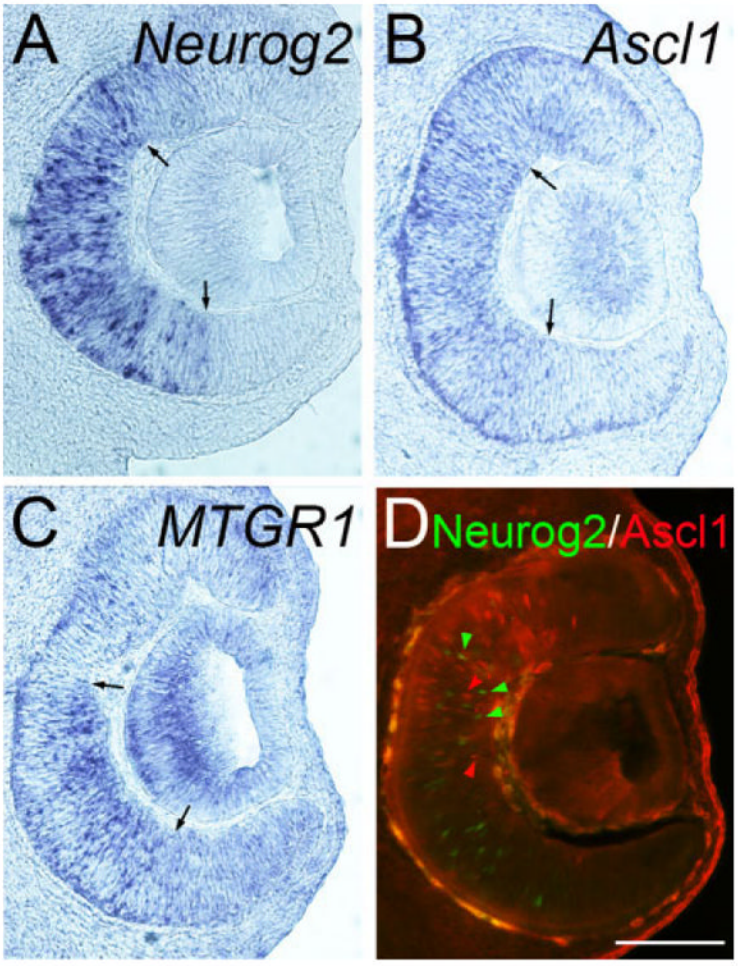

Fig. 5.

Retina at E11.5. Frontal sections of the retina at E11.5. Midline is to the left. In situ hybridization for *Neurog2* (**A**), *Ascl1* (**B**), *MTGR1* (**C**) as well as double immunohistochemistry of Ascl1 and Neurog2 (**D**) is shown. Red and green arrowheads in D indicate Neurog2-positive and Ascl1-positive cells, respectively. These two populations do not significantly overlap at this stage. Scale bar = 200 μm.

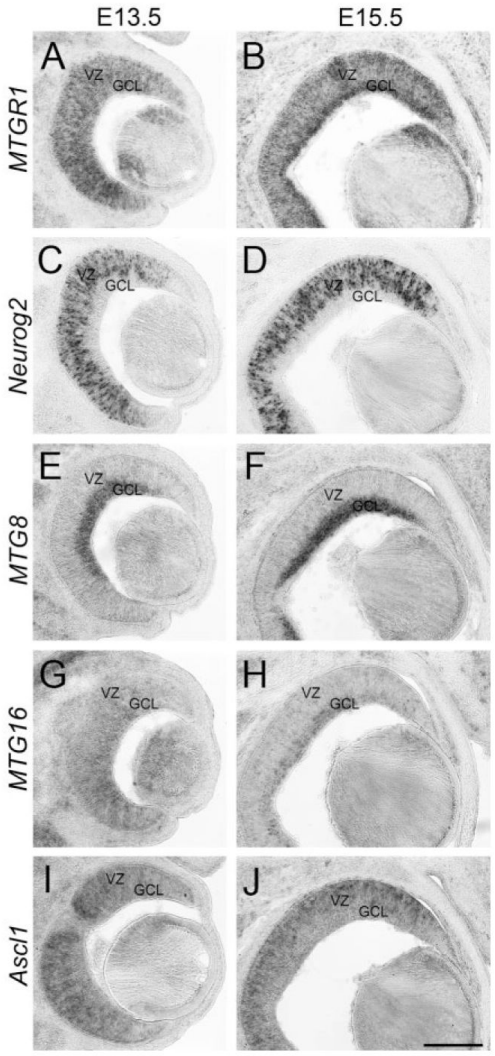

Fig. 6.

Retina at E13.5 and E15.5. Frontal sections of the forebrain at E13.5 (A,C,E,G,I) and E15.5 (B,D,F,H,J). Midline is to the left. In situ hybridization for *MTGR1* (**A,B**), *Neurog2* (**C,D**), *MTG8* (**E,F**), *MTG16* (**G,H**), and *Ascl1* (**I,J**) is shown. VZ, ventricular zone; GCL, ganglion cell layer. Scale bar = 200 μm.

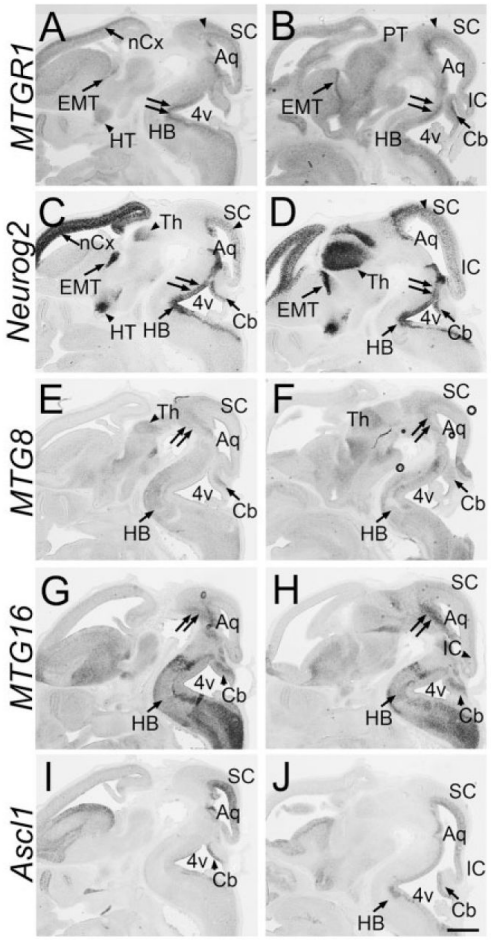

Fig. 7.

Sagittal sections at E12.5. Sagittal sections of the brain at E12.5. Front is to the left. In situ hybridization for *MTGR1* (**A,B**), *Neurog2* (**C,D**), *MTG8* (**E,F**), *MTG16* (**G,H**), and *Ascl1* (**I,J**) is shown. nCx, neocortex; Th, thalamus; EMT, eminentia thalami; HT, hypothalamus; PT, pretectum; HB, hindbrain; Aq, cerebral aquaduct; 4v, fourth ventricle; SC, superior colliculus; IC, inferior colliculus; Cb, cerebellum. Scale bar = 500 μm.

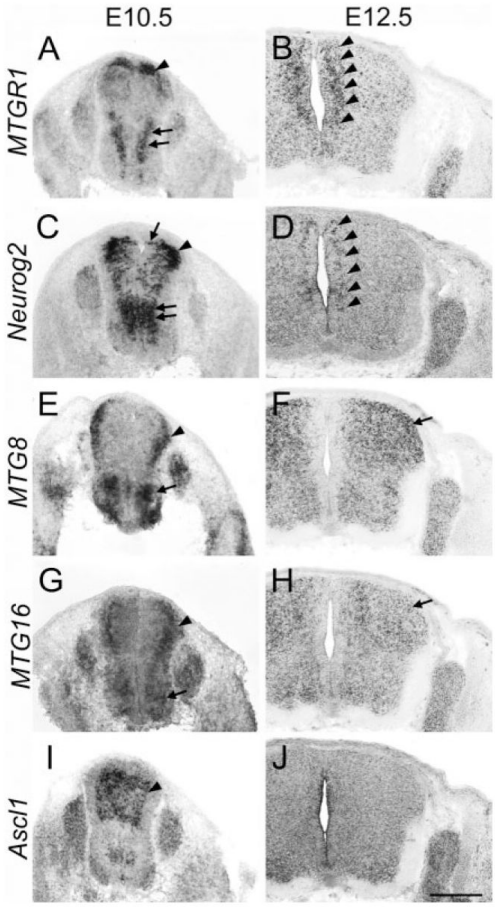

Fig. 8.

Spinal cord at E10.5 and E12.5. Transverse sections of the spinal cord at the thoracic level at E10.5 (A,C,E,G,I) and E12.5 (B,D,F,H,J). In situ hybridization for *MTGR1* (**A,B**), *Neurog2* (**C,D**), *MTG8* (**E,F**), *MTG16* (**G,H**), and *Ascl1* (**I,J**) is shown. Scale bar = 500 μm.

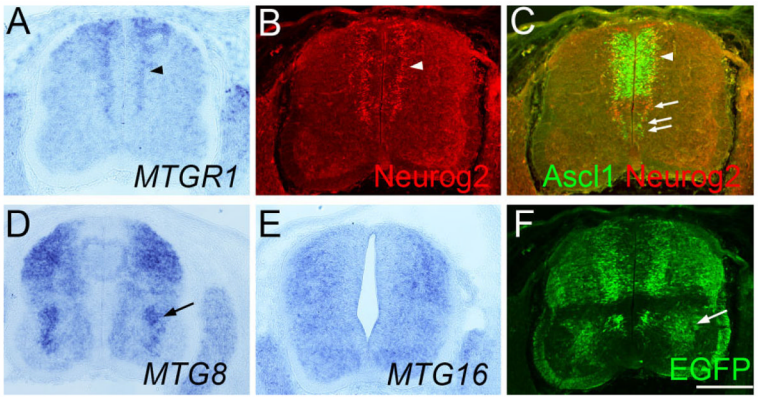

Fig. 9.

Analysis of *Ascl1-BAC-EGFP* embryos at E11.5. Transverse sections of the lumber spinal cord (**A–F**) of the same *Ascl1-BAC-EGFP* embryo at E11.5. Sections in A–F are adjacent to each other and B and C are from the same section. In situ hybridization for *MTGR1* (A), *MTG8* (D), *MTG16* (E), as well as immunostaining for Neurog2 (B), Ascl1/Neurog2 (C), and EGFP (F) is shown. Scale bar = 200 μm.